International Journal of ISSI, Vol. 14 (2017), No. 2, pp. 9-15

Corrosion Resistance and Semiconducting Properties of the Passive Films on Duplex Stainless Steel 2205

M. Ebrahimi [1], I. Danaee *[2], H. Eskandari [3], S. Nikmanesh [4]

Abadan Faculty of Petroleum Engineering, Petroleum University of Technology, Abadan, Iran

Abstract

In this study, the effect of molybdate on the electrochemical behavior and semi-conductive properties of duplex stainless steel 2205 passive film at NaCl solutions was investigated. Cyclic potentiodynamic polarization, impedance spectroscopy, mott-schottky plots and scanning electron microscopy (SEM) were used to study the passive behavior. Polarization curves showed that the corrosion current and passive current density of stainless steel decreased with increasing molybdate concentrations. Mott–Schottky analysis revealed that the passive films formed on duplex stainless steels behave as n-type and p-type semiconductors and the donor and acceptor densities reduced with increasing molybdate concentration. Electrochemical impedance spectroscopy (EIS) results showed that charge transfer and passive resistance increased in the presence of molybdate. In addition, double layer and film capacitance decreased with increasing molybdate concentration and passive film thickness increased. Scanning electron microscopy was used to study the steel surface and showed more uniform surface with lower damage in the presence of molybdate.

Keywords: Duplex stainless steel 2205; Impedance; Mott–Schottky; Semiconductive property.

1. Introduction

2205 duplex stainless steels (DSS) is a two- phase, ferritic, austenitic 22% chromium, 3 % molybdenum, 5 to 6 % nickel alloyed stainless steel [1]. DSS shows characteristic of both austenitic and ferritic stainless steels, a desirable combination of high tensile strength and fatigue strength, good toughness even at lower temperatures, adequate formability and weld ability, and excellent resistance to stress corrosion cracking and corrosion [2]. It is known that the presence of alloyed elements such as Cr, Mo, and N improves the resistance to localized corrosion of the stainless steels. Their excellent corrosion resistance results from the formation of a thin and tenacious protective film, usually less than 5 nm, due to the oxidation of the metal [2,3]. The corrosion resistance of stainless steel is related to the composition, electrochemical or semi conductive behavior of its passive film [4]. The electrochemical behavior of the passive film is related to temperature, pH, time, chemical composition of electrolyte and its semi conductive property in most cases [5–8]. Electronic properties are a significant aspect of the nature of the passive film. Moreover, electron transfer reactions that occur on the surfaces with passive films depend strongly on the electronic properties of such films.

Sato put forward the electronic properties of the passive film and classified them into n-type and p-type oxides [9]. The stability of the passive film depends on its electronic properties. The passive film of n-type oxide appears to be electrochemically more stable than that of p-type oxide against anodic polarization. Bianchi, however, found that a surface of n-type passive film counts more pits than surfaces with p-type films [10]. This protective film is strongly adherent and chemically stable. In certain environments, especially ones containing chloride, this oxide film breakdown and rapid corrosion ensues since many surface defects provide preferential sites for the initiation of localized corrosion [11].

Much work has been done to study the corrosion and passivation behaviors of the passive layers formed on some types of stainless steels. Freire et al.[12] studied the passive behavior of AISI 316 in alkaline media. Ben-Salah et al.[13] studied the passivity and corrosion resistance of a highly alloyed austenitic stainless steel (Sanicro28) in 50 wt.% H_3PO_4 industrial medium containing impurities at the temperatures of 20 °C to 80 °C after different immersion times. Results demonstrated that Sanicro28 passivates spontaneously. Influences of pH value, temperature, chloride ions and sulfide ions on the corrosion behaviors of 316L stainless steel were investigated by Li et al.[14].

Mott–Schottky plots showed that the passive films appear to be p-n heterojunctions and have highly defective character. The donor and acceptor densities increased with increasing temperature, chloride and sulfide ion concentration. In addition, a lot of research has been performed on increasing the passive resistance of

* *Corresponding author*
Email: danaee@put.ac.ir
Address: Abadan Faculty of Petroleum Engineering, Petroleum University of Technology, Abadan, Iran
1. M.Sc.
2. Associate Professor
3. Assistant Professor
4. Assistant Professor

stainless steels and its relation to increasing corrosion resistance. Jinlong et al.[15] studied the effect of cold rolling on passive and corrosion resistance of 2205 duplex stainless steel in borate buffer. The ultrafine grained sample showed higher corrosion resistance than the coarse grained solution, indicating that the passive film formed on the surface of the ultrafine grained 2205 duplex stainless steel is more protective. Mao et al.[16] investigated the effect of octadecylamine on the corrosion behavior and passive resistance of Type 316SS in acetate buffer. The results indicated that corrosion resistance and passive resistance increased with increasing octadecylamine concentration in the solution up to a limit concentration.

The aim of the present work is to investigate the effect of molybdate on increasing corrosion and passive resistance of 2205 duplex stainless steel in 3.5% sodium chloride solutions. Potentiodynamic polarization, impedance spectroscopy and mott-schottky analysis were used to study passive resistance. In addition, semi-conductive properties of passive film and donor and acceptor density were studied in the presence of molybdate.

2. Materials and Methods

The materials tested were 2205 duplex stainless steel. The composition of the tested duplex stainless steels is shown in Table 1. Samples for electrochemical experiments were cut in cubic dimensions using wire cute machine. The samples were embedded in polyester resin after establishing the electrical contact, taking special care to avoid the presence of crevices. A surface area of 1 cm^2 was exposed to the test solution. The samples were ground with emery paper up to 2000 grit before each experiment. After cleaning and rinsing with distilled water, the polished sample was instantly assembled into the measurement cell and subsequently the electrolyte was filled in the cell. The test solutions were 3.5% NaCl.

Electrochemical measurements were carried out by EG&G potentiostat model PARSTAT 2273 advanced electrochemical system coupled with a conventional three electrode cell. A saturated calomel electrode (SCE) was used in all cases. A platinum rod was used as the counter electrode and the sample prepared using the above method as the working electrode, should be prepared in accordance to ASTM G-5.

Before the experiments, samples were immersed in electrolyte for 20 min for steady state condition. The polarization curves were recorded potentiodynamically at 1mVs^{-1} using an electrochemical system, and the potential started from -1000 mVSCE. The measurements of the EIS at the open-circuit potential (OCP) were made over a frequency range of 100 kHz to 10 mHz and an amplitude of the perturbation signal of 10 mV. The measurements of Mott–Schottky plot were performed at 1000 Hz over a potential range of 300 to 1100 mV.

The surface morphology of the electrode surface was evaluated by scanning electron microscopy model VEGA, TESCAN at ×1000 magnification.

3. Results and Discussions

3.1. Cyclic polarization curve

Potentiodynamic polarization curves of steel electrode in 3.5% NaCl solution containing molybdate are depicted in Fig. 1. Inspection of the curve reveals that the anodic scan exhibits a passivation behavior prior to a certain critical breakdown potential E_b. As can be seen, a wide passive region is obtained up to +1.1 V due to the stability of passive film of 2205 duplex stainless steel.

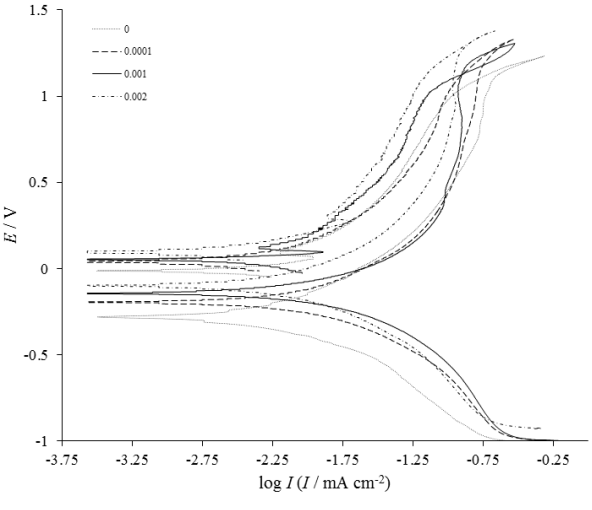

Fig. 1. Cyclic polarization curves of duplex stainless steel electrode in 3.5% Nacl solution at different concentrations of molybdate.

Similar results have been obtained in other works [15, 17]. When the critical potential E_b is exceeded an increasing current is observed indicating breakdown of the passive film at local points. For $E>E_b$, the current corresponds largely to the pitting corrosion of stainless steel. In the course of a reverse potential sweep, the anodic current density decreases very sharply and remains almost closely to the current in the anodic sweep. No considerable loop, characteristic for susceptibility to pitting corrosion phenom-

Table 1. Chemical composition of duplex AISI 2205 stainless steel.

Elements	C Max	Si Max	Mn Max	P Max	S Max	Cr	Ni	Mo	N
wt.%	0.03	1.0	2.0	0.03	0.015	22	5	3.2	0.18

enon, appears in reverse scan. The values of the relevant electrochemical parameters were extracted from the potentiodynamic polarization curves and summarized in Table 2. As can be seen, the corrosion potentials shift in the positive direction and the corrosion current decreases with increasing molybdate concentrations. Moreover, passive potential region enlarges and the passive current decreases with increasing molybdate, implying enhanced anticorrosion behaviors in the presence of molybdate. In addition, the current density of cathodic branch in polarization diagrams increases in the presence of molybdate due to the interference of molybdate in a reduction reaction. The possible reduction reaction of MoO_4^{2-} occurring on the electrode surface is as follows [18]:

$$MoO_4^{2-} + 4H^+ + 2e \rightarrow MoO_2 + 2H_2O \quad (1)$$

The reduction of the molybedate anion could provide additional oxygen anions that interfere with the ability of Cl^- anion to reach the metal/film interface, possibly by blocking sites through which aggressive anions preferentially defuse to the film. Sugimoto[19] found that molybdate ions preferentially adsorb on the steel surface and preclude the adsorption of Cl^- ions. can also act the following reactions:

$$MoO_4^{2-} + H^+ \rightarrow MoO_3(OH)^- \quad (2)$$

$$2MoO(OH)_5^- \rightarrow \left[(OH)_4\,OMo\text{-}O\text{-}MoO(OH)_4\right]^{2-} + H_2O \quad (3)$$

Molybdenum oxide has the ability to corporate in passive layer and fills the defect[19] which leads to increasing passive compactness with a greater protective ability to obstruct the permeation of the aggressive ions into the passive film. In addition, the tendency of molybdate to reduction leads to increasing steel oxidation and passive production. Thus, the corrosion resistance is strengthened.

3. 2. Electrochemical impedance

In order to get more information about the corrosion phenomenon, the impedance measurements have been carried out in different concentration of molybdate. The impedance plot for steel electrode in 3.5 % NaCl solutions with different molybdate concentrations at open circuit potential is shown in Fig. 2. The data revealed that the impedance diagram consists of two overlapped

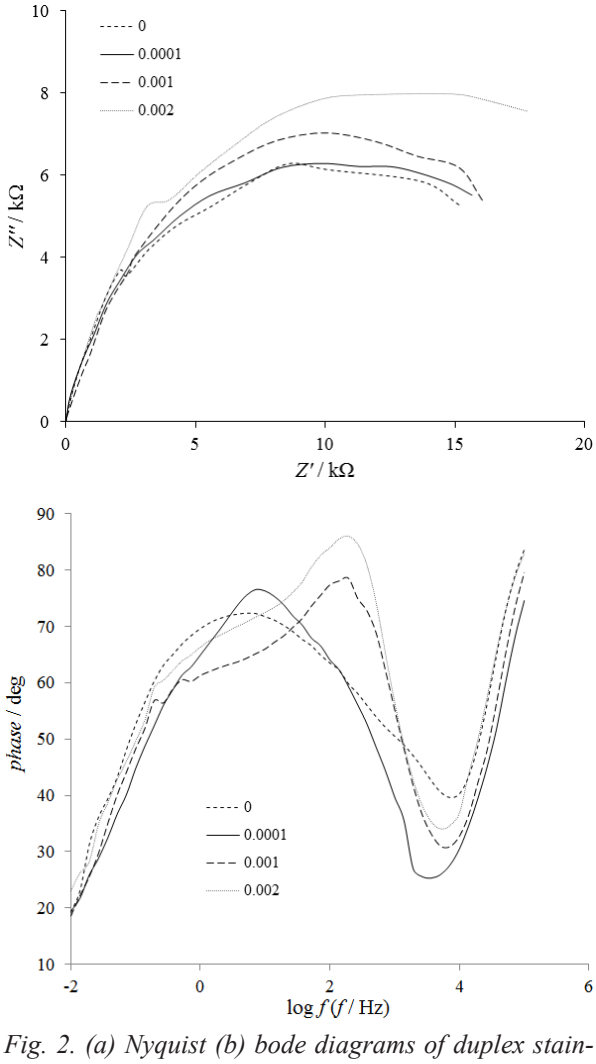

Fig. 2. (a) Nyquist (b) bode diagrams of duplex stainless steel electrode in 3.5% NaCl solution at different concentrations of molybdate.

Table 2. Cyclic polarization parameters for corrosion of duplex AISI 2205stainless steel in 3.5% NaCl solution at different concentrations of molybdate.

Molybdate Concentration / M	E_{corr} / mV	E_{pit} / mV	I_{corr} / μA cm^{-2}	C. R / mm year^{-1}
0	-284.9	1130	2.743	0.008975
0.0001	-199.2	1190	2.625	0.00859
0.001	-141.8	1201	2.428	0.007944
0.002	-104.1	1267	2.197	0.007189

capacitive semicircles which were depressed towards the real axis (Fig. 2a). The depressed semicircle in the low frequency region can be related to the combination of charge transfer resistance and the double layer capacitance. The high frequency semicircle is attributed to capacitive behavior of the passive film, coupled with a resistance due to the ionic paths through the oxide film. A broad peak is observed in the Bode plots corresponding to two overlapped semicircles in the Nyquist plot (Fig. 2b). These two overlapped semicircles are the characteristic of the passive film on stainless steels [14]. The equivalent circuit compatible with the impedance diagrams is depicted in Fig. 3. In this electrical

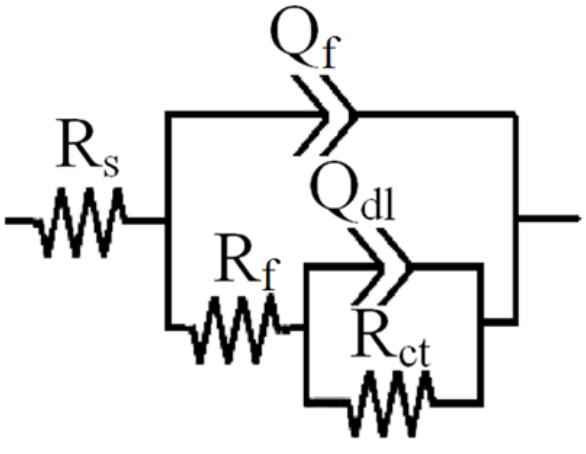

Fig. 3. Equivalent circuits compatible with the experimental impedance data in Fig. 2 for corrosion of duplex steel alloy electrode in NaCl solution.

equivalent circuit, R_s, Q_{dl} and R_{ct} represent solution resistance, a constant phase element corresponding to the double layer capacitance and the charge transfer resistance of dissolution reaction. CPE_f and R_f are the electrical elements related to the resistance and capacitance of the passive film. To obtain a satisfactory impedance simulation of duplex stainless steel, it is necessary to replace the capacitor (C) with a constant phase element *(CPE) Q* in the equivalent circuit. The most widely accepted explanation for the presence of *CPE* behavior and depressed semicircles on solid electrodes is microscopic roughness, causing an inhomogeneous distribution in the solution resistance as well as in the double-layer capacitance [14]. The simplest approach requires the theoretical transfer function $Z(\omega)$ to be represented by:

$$Z(\omega) = R_s + \frac{R_f}{1+\left(Z_{ct}(\omega)/R_f\right)+(i\omega)^{n_1} R_f Q_f}$$

$$Z_{ct}(\omega) = \frac{R_{ct}}{(i\omega)^{n_2} Q_{dl} R_{ct} + 1} \qquad \text{Eq. (4)}$$

ω is the frequency in rad/s, $\omega = 2\pi f$ and f is frequency in Hz. To corroborate the equivalent circuit, the experimental data are fitted to equivalent circuit and the circuit elements are obtained. Table 3 illustrates the equivalent circuit parameters for the impedance spectra of duplex steel corrosion in NaCl solution. From Table 3 with increasing molybdate concentration, the charge transfer and passive resistanceincrease. Higher Rf and Rct values reflect the decrease in the porosity of passive film due to the protective properties of molybdate on the surface. Q_{dl} can be easily calculated based on the equivalent circuit of the measured EIS. It appears that the double layer and film capacitance tend to decrease as the molybdate concentration increases. The passive film thickness (d) can be calculated using the Eq. (5) [14]

$$d = \frac{\varepsilon\varepsilon_o A}{C} \qquad \text{Eq. (5)}$$

, where ε_0 is the vacuum permittivity (8.854×10^{-14} F cm^{-1}), ε_f is the dielectric constant of the passive film. Generally, a change in the capacitance of the passive film can be used as an indicator for change in the passive film thickness. As can be seen from Eq. (5), passive film thickness increases with increasing molybdate concentrations. This leads to forming the passive films with higher protection behavior, due to the growth of much thicker and less defective passive films [14].

3. 3. Mott-Schottky

The semi-conductive parameters of the passive films on metals are often obtained using the Mott-Schottky analysis. The charge distribution at the semiconductor/solution is usually determined based on Mott–Schottky relationship by measuring the electrode capacitance as a function of electrode potential E [20-22]:

$$\frac{1}{C^2} = \frac{2}{\varepsilon\varepsilon_o e N_D}\left(E - E_{fb} - \frac{kT}{e}\right) \qquad \text{Eq. (6)}$$

For n- type semiconductor

$$\frac{1}{C^2} = \frac{-2}{\varepsilon\varepsilon_o e N_A}\left(E - E_{fb} - \frac{kT}{e}\right) \qquad \text{Eq. (7)}$$

For p- type semiconductor

, where ε is the dielectric constant of thepassive film, ε_o the permittivity of vacuum (8.854×10^{-12} F/m), e the electron charge, N_D the donor density for n-type semiconductor and the accepter density for p-type semiconductor, E_{fb} the flat band potential, k the Boltzmann constant and T is the absolute temperature. According to Eqs. (5) and (6), N_D and N_A can be determined from the slope of the experimental $1/C^2$ versus E plots, and E_{fb} from the extrapolation of the linear portion to $1/C^2 = 0$.

Fig. 4 shows the Mott-Schottky plots of the passive films on duplex stainless steel in 3.5% Nacl solution with different concentration of molybdate. It should be noted that for all concentrations, capacitances decreases clearly with increasing molybdate concentration. All plots show three regions in which a linear relationship between C^{-2} and E can be observed. The negative slopes in region I can be attributed to a p-type behavior. Region II presents positive slopes, depicting an n-type semiconducting behavior. Finally, the negative slopes in region III can be attributed to p-type behavior. This feature is usually explained in terms of a strong dependence of the Faradaic current on potential in the transpassive region[23]. In this sense, the behavior of capacitance at high potentials near the transpassive region is attributed to the development of an inversion layer as a result of an increasing concentration in the valence band (high valency Cr in the film prior to transpaasive dissolution).

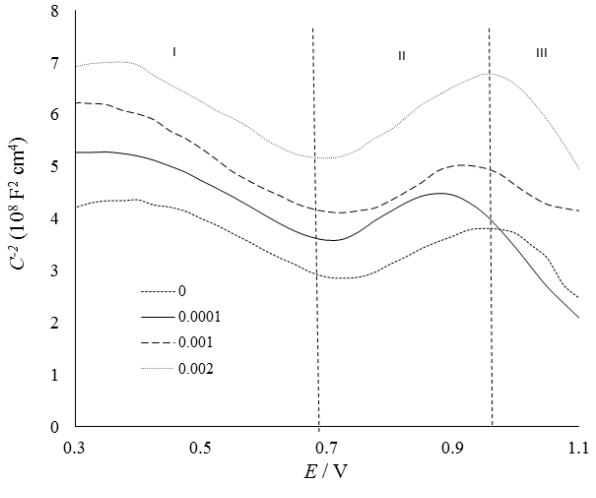

Fig. 4. Mott–Schottky plots of the capacitance behavior of the passive film for duplex steel electrode in 3.5% NaCl solution at different concentrations of molybdate.

For the potential regions of more than 0.7 V, the positive slope indicates n-type behavior and in potentials less than 0.7 V, the negative slope is representative of a p-type semiconductor. Thus, Mott-Schottky analysis shows that the passive films behave as n-type and p-type semiconductors above and below the flat band potential respectively. This behavior implies that the passive films could have a duplex structure. Early studies of the bipolar duplex structures of passive films on stainless steels are attributed to Sato [24]. In addition, exact investigation of passive film needs X-ray photoelectron spectroscopy. Jinlong et al. [15] studied the passive structure of ultrafine grained duplex AISI 2205 stainless steels and indicated two parts of passive film with different compositions. Lv et al. [25] investigated the passive structure of sensitized duplex AISI 2205stainless steels by X-ray photoelectron spectroscopy and Mott-Schottky analysis. The results indicated chromium oxides and iron oxides in different parts of the passive film. Luo et al. [26] studied the passivation behavior of 316L stainless steels and the same results were obtained. It is widely accepted that the inner part of the passive film, which has a p-type behavior, consists mainly of Cr oxides, whereas the outer region, with the features of an n-type behavior, is predominantly Fe oxides. Contributions to the p-type behavior at $E < E_{fb}$ are restricted to the inner Cr oxide layer, with negligible contributions from the Fe oxides in the outer part of the film, whereas the n-type behavior at $E > E_{fb}$ depends exclusively on the outer Fe oxide region with low contribution from the Cr oxide region [27]. According to Point Defect Model PDM [5], the n-type semi-conductive character of the passive film indicates that the dominant defect in the passive film over the potential region II is oxygen vacancies or metal interstitials, and cation vacancies may be the dominant defects in the passive films over potential regions I and III. In addition, the donor density N_D characterizes the affinity of chloride ions for the passive film and also features the pit nucleation ability.

The variations in the slopes of the $C^{-2} \sim E$ plots with the sweep potential are often attributed to the compositions and structures of the passive films [28]. The presence of molybdate raises the Mo content in the passive oxide layer [29, 30]. MoO_4^{2-} anions neutralize the positive donors, decrease the conductivity, and possibly repel the chloride adsorption to increase the corrosion resistance of stainless steels [29]. So, with increasing molybdate concentrations, the doping densities decrease, which is related to the decrease of the number of point defects on the film. Moreover, it is suggested that the space charge layer thickens with the chromium content, leading to higher resistance since chromium acts as a barrier to the flow of the electrons and holes. The parameters were calculated and showed in Table 3. As can be seen, NA

Table 3. Impedance parameters obtained in 3.5% NaCl solutions with different concentrations of molybdate at open-circuit potential.

molybdate concentration (M)	R_s / Ω cm^2	R_f / Ω cm^2	$Q_f \times 10^4$ / Ω^{-1} s^n cm^{-2}	n_f	$R_{ct} \times 10^{-4}$ / kΩ cm^2	$Q_{dl} \times 10^4$ / Ω^{-1} s^n cm^{-2}	n_{dl}
0	2.5	115	3.5	0.78	1.92	5	0.7
0.0001	2.1	135	3	0.83	2.04	3.8	0.68
0.001	1.9	152	2.8	0.88	2.07	3.3	0.72
0.002	1.8	204	2.2	0.92	2.52	3.2	0.7

and ND decrease with increasing molybdate, implying the decreased defect density in the outer and inner films with increase in molybdate concentrations. The decrement of defect of the inner and outer films implies the enhanced compactness and homogenous character of the passive film [28]. According to Larkin [30], molybdate ions act as an electron acceptor in which when adsorbed on the surface of the passive film, would strengthen the metal-oxygen bonds of the film. This is in agreement with the obtained data from potentiodynamic polarization and decreasing passive and corrosion current density in the presence of molybdate. Moreover, the charge transfer and passive resistance increase and capacitance behavior of passive decreases in the presence of molybdate due to decreasing in doping and defect density of the film. Eghbali et al. [11] studied the effect of molybdate on pitting corrosion behavior and critical pitting temperature of duplex AISI 2205 stainless steel. Theresults indicated that the pitting corrosion resistance and critical pitting temperature increased in the presence of molybdate. This is in agreement with decreasing the donor density which is susceptible for chloride attack.

The flat band potential (E_{FB}) is a critical parameter which is used to determine the positions of the semi-conductive energy bands with respect to the redox potentials of electro active ions in the solution [28]. Table 3 shows that E_{FB} shifts to the positive direction with increasing molybdate, suggesting the increment of the passive film stability.

3. 4. SEM

In order to evaluate the conditions of the steel surfaces in contact with corrosive solution, surface analysis was carried out. Scanning electron microscopy was carried out after applying 1 V potential versus reference electrode 3.5% NaCl for 1200 s. SEM images of the surface in the absence and presence of molybdate are presented in Fig. 5. SEM reveals the presence of corrosion attack and some pits on the surface in the absence of Na_2MoO_4 while such damages are diminished in the presence of Na_2MoO_4. As can be seen from these figures, it is obvious that the surface looks more uniform in the presence of Na_2MoO_4.

4. Conclusions

The corrosion behavior and passive resistance of duplex AISI 2205 stainless steel was investigated in NaCl solution in the presence of molybdate. The following conclusions were obtained:

- The corrosion and passive current decreased in the presence of molybdate due to the increasing protective ability of the passive film.
- Impedance spectroscopy indicated that charge transfer and passive resistance increased with increasing molybdate concentrations. Also, EIS results showed that increasing molybdate concentrations offers better conditions for forming the passive films with higher

Table 4. The donor density, accepter density and the flat band potential of the passive film formed on duplex AISI 2205 stainless steel in 3.5% NaCl solution at different concentrations of molybdate.

Molybdate Concentration / M	N_D /10^{22} cm^{-3}	N_A /10^{22} cm^{-3}	E_{fb-n} / V	E_{fb-n} / V
0	1.653	2.434	0.205108	1.221044
0.0001	1.316	2.316	0.175634	1.311435
0.001	1.277	2.189	0.123065	1.301458
0.002	1.204	1.885	0.0108446	1.436919

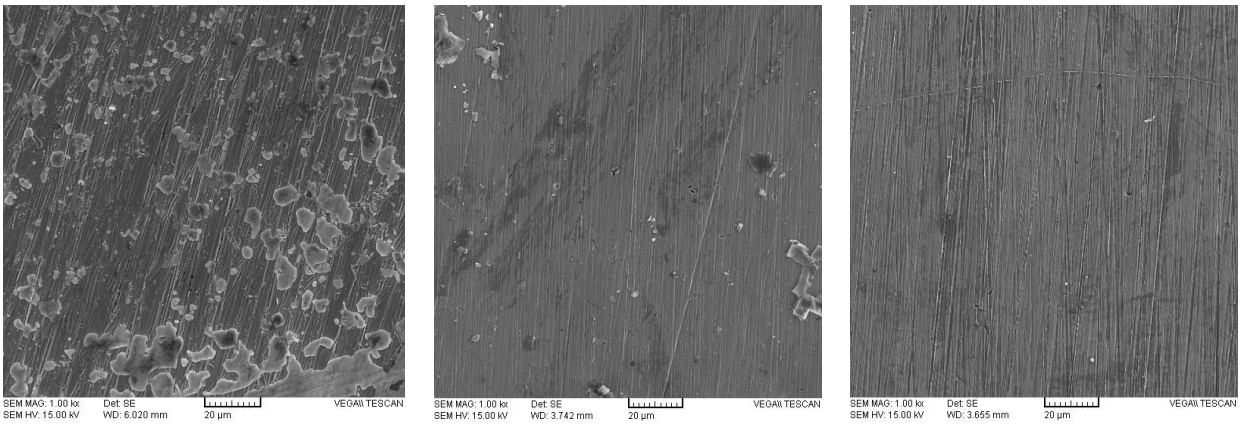

Fig. 5. Surface of duplex steel alloy electrode by SEM after applying 1 V anodic potential versus the reference electrode in NaCl solution at different concentrations of molybdate: a) 0, b) 0.001 and c) 0.002 M.

protection behavior, due to the growth of much thicker and less defective films.

• Mott–Schottky analysis revealed that the passive films formed on duplex AISI 2205 stainless steel behave as n-type and p-type semiconductors and the donor and acceptor densities decreased with increasing molybdate concentrations.

• The scanning electron microscopy micrographs showed that the corrosion attack decreased in the presence of molybdate.

References

[1] A. Igual Muñoz, J. García Antón, S. López Nuévalos, J. L. Guiñón and V. Pérez Herranz: Corros. Sci., 46(2004), 2955.
[2] H. Luo, C. F. Dong, K. Xiao and X. G. Li: Appl. Surf. Sci., 258(2011), 631.
[3] R. M. Fernández-Domene, E. Blasco-Tamarit, D. M. García-García and J. García-Antón: Electrochim. Acta., 95(2013), 1.
[4] H. Luo, H. Su, C. Dong, K. Xiao and X. Li: Data Br., 5(2015), 171.
[5] H. Li, Z. Jiang, H. Feng, S. Zhang, P. Han, W. Zhang and G. Li: Int. J. Electrochem. Sci., 10(2015), 4832.
[6] J. Huang, X. Wu and E.-H. Han: Corros. Sci., 51(2009), 2976.
[7] S. Jin and A. Atrens: Appl. Phys. A Solids Surf., 42(1987), 149.
[8] H.-H. Ge, X.-M. Xu, L. Zhao, F. Song, J. Shen and G.-D. Zhou: J. Appl. Electrochem., 41(2011), 519.
[9] N. Sato: J. Electrochem. Soc., 129(1982), 255.
[10] G. Bianchi, A. Cerquetti, F. Mazza and S. Torchio: Corros. Sci., 12(1972), 495.
[11] F. Eghbali, M. H. Moayed, A. Davoodi and N. Ebrahimi: Corros. Sci., 53(2011), 513.
[12] L. Freire, M. J. Carmezim, M. G. S. Ferreira and M. F. Montemor: Electrochim. Acta., 55(2010), 6174.
[13] M. BenSalah, R. Sabot, E. Triki, L. Dhouibi, Ph. Refait and M. Jeannin: Corros. Sci., 86(2014), 61.
[14] D.G. Li, J.D. Wang, D.R. Chen and P. Liang: J. Power Sources., 272(2014), 448.
[15] L. Jinlong, L. Tongxiang, W. Chen and D. Limin: J. Electroanal. Chem., 757(2015), 263.
[16] F. Mao, C. Dong and D. D. Macdonald: Corros. Sci., 98(2015), 192.
[17] Y. S. Kim: Met. Mater., 4(1998), 183.
[18] G.O. Ilevbare and G.T. Burstein: Corros. Sci., 45(2005), 1545.
[19] K. Sugimoto and Y. Sawada: Corrosion, 32(1976), 347.
[20] M. D. Krotova, Yu. V. Pleskov, A. A. Khomich, V. G. Ralchenko, D. N. Sovyk and V. A. Kazakov: Russ. J. Electrochem., 50(2014), 101.
[21] F. La Mantia, H. Habazaki, M. Santamaria and F. Di Quarto: Russ. J. Electrochem., 46(2010), 1306.
[22] J. Ding, L. Zhang, M. Lu, J. Wang, Z. Wen and W. Hao: Appl. Surf. Sci., 289(2014), 33.
[23] C. Escrivà-Cerdán, E. Blasco-Tamarit, D.M. García-García, J. García-Antóna and A. Guenbour: Electrochim. Acta, 80(2012), 248.
[24] N. Sato: Corros. Sci., 31(1990), 1.
[25] J. Lv, T. Liang, C. Wang and T. Guo: J. Alloys Comp., 658(2016), 657.
[26] H. Luo, H. Su, C. Dong and X. Li: Appl. Surf. Sci., 400(2017), 38.
[27] E.E. Oguzie, J. Li, Y. Liu, D. Chen, Y. Li, K. Yang and F. Wang: Electrochim. Acta., 55(2010), 5028.
[28] D. G. Li, J. D. Wang, D. R. Chen and P. Liang: Int. J. Hydrogen Energy., 40(2015), 5947.
[29] W. J. Tobler: Influence of molybdenum species on pitting corrosion of stainless steels, Doctoral thesis of Swiss Federal Institute of Technology in Zurich (ETHZ), 2004.
[30] B. M. Larkin and I. L. Rozenfeld: Prot. Metals., 17(1981), 408.